Tyrosine phosphorylation modulates cell surface expression of chloride cotransporters NKCC2 and KCC3

Cláudia Almeida Loureiro[a,b], Patrícia Barros[a,b], Paulo Matos[a,b,c], Peter Jordan[a,b]

[a] Department of Human Genetics, National Health Institute 'Dr. Ricardo Jorge', Lisbon, Portugal;

[b] BioISI - Biosystems & Integrative Sciences Institute, Faculty of Sciences, University of Lisbon,

[c] Department of Chemistry and Biochemistry, Faculty of Sciences, University of Lisbon.

*Corresponding author: Dr. Peter Jordan, Departamento de Genética Humana, Instituto Nacional de Saúde Doutor Ricardo Jorge, Avenida Padre Cruz, 1649-016 Lisboa, Portugal. Telephone: +351-21-7519380;

E-mail: peter.jordan@insa.min-saude.pt.

Declarations of interest: none.

Abstract

Cellular chloride transport has a fundamental role in cell volume regulation and renal salt handling. Cellular chloride entry or exit are mediated at the plasma membrane by cotransporter proteins of the solute carrier 12 family. For example, NKCC2 resorbs chloride with sodium and potassium ions at the apical membrane of epithelial cells in the kidney, whereas KCC3 releases chloride with potassium ions at the basolateral membrane. Their ion transport activity is regulated by protein phosphorylation in response to signaling pathways. An additional regulatory mechanism concerns the amount of cotransporter molecules inserted into the plasma membrane. Here we describe that tyrosine phosphorylation of NKCC2 and KCC3 regulates their plasma membrane expression levels. We identified that spleen tyrosine kinase (SYK) phosphorylates a specific N-terminal tyrosine residue in each cotransporter. Experimental depletion of endogenous SYK or pharmacological inhibition of its kinase activity increased the abundance of NKCC2 at the plasma membrane of human embryonic kidney cells. In contrast, overexpression of a constitutively active SYK mutant decreased NKCC2 membrane abundance. Intriguingly, the same experimental approaches revealed the opposite effect on KCC3 abundance at the plasma membrane, compatible with the known antagonistic roles of NKCC and KCC cotransporters in cell volume regulation. Thus, we identified a novel pathway modulating the cell surface expression of NKCC2 and KCC3 and show that this same pathway has opposite functional outcomes for these two cotransporters. The findings have several biomedical implications considering the role of these cotransporters in regulating blood pressure and cell volume.

Keywords

chloride cotransport, KCC3, NKCC2, membrane traffic, protein phosphorylation, SYK,

Abbreviations

FBS- fetal bovine serum; KCC3- K-Cl cotransporter (KCC) isoform 3; NKCC2- Na-K-Cl cotransporter (NKCC) isoform 2; siRNA- small interfering RNA; SLC12- solute carrier family 12; SYK- spleen tyrosine kinase; wt- wild type

1. Introduction

Cellular chloride transport plays important roles in the maintenance of cell volume, the regulation of blood pressure, and in neuronal excitability (Kahle et al. 2006; Pedersen et al. 2013; Watanabe and Fukuda 2015). One important family of plasma membrane proteins that mediate chloride entry into or exit from cells are the cotransporters of the solute carrier 12 family. Their activity remains electroneutral because Cl^- is cotransported with either Na^+ and/or K^+ ions and the driving force is the electrochemical gradient established by the ATP-dependent Na^+/K^+–ATPase. Two phylogenetic and functional subgroups exist in the SLC12 family: the genes *SLC12A1 –A3* encode $Na^+/K^+/Cl^-$ cotransporters required for Cl^- entry into cells, while the *SLC12A4-A7* genes encode K^+/Cl^--cotransporters mediating Cl^- exit (Arroyo et al. 2013).

The SLCA1-A3 members are known as NKCC2, NKCC1 and NCC, respectively. NKCC2 is an apical cotransporter mostly expressed in the thick ascending limb of the loop of Henle (TAL) and the *macula densa* of the proximal nephron, and is a key mediator of renal Na^+ and Cl^- reabsorption (Gamba and Friedman 2009; Ares et al. 2011). Its specific inhibition by diuretic drugs such as bumetanide or furosemide is used to treat high blood pressure. NKCC1 is ubiquitously expressed to assure cell volume regulation. Its basolateral Cl^- entry activity is further important in sustaining apical Cl^- secretion in certain epithelia. NCC is found in the apical membrane of Cl^--resorbing cells of the distal convoluted tubule of the nephron (McCormick et al. 2008; Moes et al. 2014). Mutations in the NKCC2 or NCC genes cause the rare genetic diseases Bartter (type I) or Gitelman syndromes characterized by low blood pressure and renal NaCl wasting (Kleta and Bockenhauer 2006; Esteva-Font et al. 2012).

On the other hand, the *SLC12A4-A7* genes encode the K^+/Cl^- cotransporters KCC1-KCC4, which move Cl^- out of cells. KCC1 is ubiquitously expressed and important for general cell volume regulation. While KCC2 is neuron-specific, KCC3 and KCC4 are both expressed in neurons and the kidney, where KCC3 is specifically expressed in the proximal tubule. Inherited mutations in the KCC3 gene or its disruption in mouse models cause peripheral neuropathy (Howard et al. 2002; Kahle et al. 2016).

Of great importance for cellular homeostasis is the synchronized activity of both subgroups within the same cell. For example, during cell volume regulation, the cell shrinkage caused by osmotic stress is counteracted by activating Cl^- entrance through

NKCC and simultaneously inhibiting Cl^- exit via KCC activity. Also, epithelia that reabsorb or secrete Cl^-, such as the kidney or lungs, respectively, require synchrony between apical and basolateral Cl^- transport activities. This requires the existence of regulatory mechanisms that act simultaneously upon NKCC and KCC cotransporters, but with opposite functional outcome, and this has been particularly well-documented in neurons (Adragna et al. 2015; Zhang et al. 2016).

One such mechanism that regulates the activity of SLC12 cotransporters in opposite ways involves their post-translational modification by protein kinases: while phosphorylation activates NKCC cotransporters (Vitari et al. 2006; Richardson et al. 2011), it inhibits KCCs (Kahle et al. 2006, 2015). Responsible for this phosphorylation are the highly homologous kinases SPAK (Ste20/SPS1-related proline- and alanine-rich kinase) and OSR1 (or oxidative stress-responsive kinase) (Piechotta et al. 2002). Both contain a conserved carboxyl (C)-terminal domain, which specifically recognizes an amino (N)-terminal RFxV/I motif in the peptide sequences of SLC12A members, for example $R^{20}FQV$ in NKCC2 and $R^{14}FMV$ in KCC3a. This interaction allows binding and subsequent phosphorylation of the cotransporters at distinct threonine (Thr) residues, for example, at Thr95, 100 and 105 in NKCC2, and at Thr991 and Thr1048 in KCC3 (Rinehart et al. 2009; de los Heros et al. 2014). In cells, endogenous KCC3 phosphorylation at Thr991 and Thr1048 is strongly reduced when cells are exposed to hypotonic conditions, and experimentally induced dephosphorylation at these sites activates ion transport by KCC3.

SPAK and OSR1, in turn, are activated by members of the WNK protein kinase subfamily (Veríssimo and Jordan 2001), which phosphorylate critical Thr residues within the T-loop motif of the catalytic domain, namely SPAK Thr233 or OSR1 Thr185 (Vitari et al. 2005; Zagórska et al. 2007). WNK kinases were proposed to act as upstream sensors of intracellular Cl^- levels since structural analysis revealed a Cl^--binding pocket around the activation loop motif DLG of the WNK catalytic domain (Piala et al. 2014; Terker et al. 2016). Other physiologic stimuli leading to activation of the WNK-SPAK/OSR1 pathway for renal chloride uptake regulation are hormones. Whereas angiotensin II stimulates NCC (Castaneda-Bueno et al. 2012), vasopressin stimulates NKCC2-mediated ion transport (Kim et al. 1999; Giménez and Forbush 2003; Welker et al. 2008; Saritas et al. 2013).

Besides cotransporter phosphorylation, another post-translational mechanism exists to rapidly regulate the cellular ion transport capacity: the amount of cotransporter protein present at the cell surface. Although membrane protein levels at the cell surface also depend on the delivery rate of newly synthesized protein, the effective balance between endocytosis and recycling of internalized transporter protein back to the cell surface can assume important regulatory roles, for example in insulin-stimulated glucose uptake (Leto and Saltiel 2012). When studied in the TAL, only around 5% of total NKCC2 protein was located at the apical membrane under basal conditions (Ares et al. 2011). In the kidney, vasopressin stimulates salt retention through NKCC2 at various levels, including protein trafficking to the cell surface (Ares et al. 2011; Castrop and Schießl 2014). These effects are mediated by the second messenger cyclic AMP (cAMP) and NKCC2 surface levels also increased after exposing isolated TAL tubules to cAMP (Giménez and Forbush 2003; Ortiz 2006)). The latter involves NKCC2 phosphorylation by protein kinase A (PKA) at Ser130 and Ser879 (Gunaratne et al. 2010) and experiments using the PKA inhibitor H-89 showed a decrease in the abundance of apical NKCC2 (Caceres et al. 2009). The cAMP-stimulated NKCC2 surface delivery in TALs was proposed to occur from intracellular storage vesicles (Giménez and Forbush 2003; Ortiz 2006) and be mediated by the vesicle-associated membrane protein 2 (VAMP2) (Caceres et al. 2014); however, the molecular mechanisms regulating the cell surface abundance are poorly understood. In the case of KCC3, about 60% of total KCC3 was detected at the plasma membrane of HEK293 cells under isotonic conditions, with the majority of this fraction being phosphorylated at Thr991 and Thr1048 and thus inactive (Rinehart et al. 2009).

A novel mechanism to modulate ion transport was recently described for the Cl^- channel cystic fibrosis transmembrane conductance regulator (CFTR), which when mutated leads to a deregulated epithelial fluid transport, namely in the lung, causing the genetic disease cystic fibrosis. Spleen tyrosine kinase (SYK) was found to regulate CFTR surface abundance through phosphorylation of Tyr512 in the nucleotide-binding domain 1 (NBD1) of CFTR (Mendes et al. 2011). In human airway epithelial cells, downregulation of endogenous SYK or overexpression of catalytically active SYK confirmed its regulatory role. Here, we describe that protein kinase SYK also phosphorylates the cotransporters NKCC2 and KCC3 within their N-terminal cytoplasmic domains. This resulted in the modulation of their cell surface abundance,

however, with opposite functional consequences: phosphorylation decreased NKCC2 but increased KCC3 levels at the cell surface.

2. Materials and Methods

2.1. Cell culture and transfections

MMDD1 (mouse macula densa-derived-1) cells (gift from K. Mutig, Charité, Berlin), and HEK293 (human embryonic kidney) cells were maintained in Dulbecco's minimal essential medium (DMEM) supplemented with 10% (v/v) fetal bovine serum (FBS) (Invitrogen). Human kidney 2 cells (HK-2) were a gift from M.J. Valente, REQUIMTE, Portugal and maintained in Dulbecco's modified eagle medium/nutrient mixture F-12 (DMEM/F12) supplemented with 10% FBS. All cells were regularly checked for absence of mycoplasm infection. For cell polarization, MMDD1 cells were grown on transwell, collagen IV-coated porous (0.4 μm) PET filter inserts (6-well size with 24.5 mm diameter, from Corning) in medium supplemented with 2.5% FBS for 10-15 days, until they reached a transepithelial electrical resistance (TEER) of ≥600Ω, as measured with a Chopstick Electrode (STX2 from WPI®) (Matos et al. 2018).

For ectopic expression of complementary DNA-encoding plasmids, HEK293 cells were transfected at 80-90% confluence using Metafectene (Biontex, Germany) according to the manufacturer's instructions. Transfection efficiencies were found to be around 90%, as determined microscopically using a GFP-encoding expression vector. The amount of transfected plasmid DNA was kept constant at 8 μg per 60 mm-dish, or 4 μg per 35 mm-dish, and adjusted with empty vector if required. Cells were analyzed after 20 h for biochemical assays.

For downregulation of endogenous proteins, 200 pmol of the corresponding small interfering RNAs (siRNAs) were transfected into HEK293 cells at 70% confluence using LipofectAMINE 2000 (Invitrogen) and cells were analyzed 48 h after transfection. siRNAs used were sc-29501 (Santa Cruz Biotechnology) against SYK and the control

luciferase GL2 siRNA (siLUC) (5'-CGU ACG CGG AAU ACU UCG ATT) (Eurofins Genomics, Germany).

For drug treatments, cells were incubated for 1 h with the vehicle DMSO (Sigma Aldrich) or with one of two different SYK inhibitors: BAY 61-3606 (2-(7-(3,4-dimethoxyphenyl)-imidazol[1,2-c]pyrimidin-5-ylamino) nicotinamide) (Calbiochem) or PRT062607 (P505-15,BIIB057) (Selleckchem) at a final concentration of 8 nM, 7 nM and 1 nM, respectively. The stock solutions were prepared at least 1000-fold in DMSO.

For challenging cell volume regulation, HEK293 were co-transfected and drug-treated as above. Cells were transferred to pre-warmed isotonic medium (10 mM HEPES, pH 7.5, 135 mM NaCl, 2 mM KCl, 2 mM $CaCl_2$, 2 mM $MgCl_2$, 1 mM KH_2PO_4, 10 mM glucose, 20 mM mannitol), imaged at marked positions under a phase contrast microscope equipped with a digital camera, then washed and incubated for 10 min in pre-warmed hypertonic medium (isotonic medium containing 220 mM mannitol) before imaging the same microscopic fields again. Digital images were analyzed using the Image J software to calculate the area covered by individual cells, as an estimate for changes in cell dimension due to shrinkage. For each data point, at least 50 cells were measured in three independent microscopic fields from three independent assays.

2.2. DNA plasmids and constructs

NKCC2 cotransporter was amplified by polymerase chain reaction (PCR) from mouse cDNA clone 4236020 (IRAVp968F0329D) (Source Bioscience, UK) with primers Eco RI-F (5' GAA TTC TCG GTC AGC ATC CCT TCC) and XhoI-R (5' CTC TTA AAG CCT GAA GGA TGC TCG AG), cloned into pCR2.2 TOPO-TA vector, and then subcloned into the Eco RI and Xho I-sites of pcDNA3-Myc vector. KCC3 cotransporter was amplified from human cDNA clone 4826538 (Source Bioscience) by PCR with primers Eco RI-F (5' ATG AGT GAG ATG T CT GGG G) and XhoI-R (5' GTG ATC ACC ATT TAT TCA TAA), cloned into pCR2.2 TOPO-TA vector, and then subcloned as an Eco RI/ Not I fragment into pcDNA3-Myc vector. NKCC2-Nterm (nucleotides 33-486) was amplified from pcDNA3-Myc-NKCC2 with primers NKCC2-F (5' GAT TCA GTG CCC AGT AAT ACC AAT CG) and NKCC2-R (5' ACG GTG ATG GGA TAC C TG GAG ATG AA); KCC3-Nterm (nucleotides 4-405) was amplified from pcDNA3-Myc-KCC3 with the primers KCC3-F(5' AGT GAG ATG TCT GGG GCC ACC A) and KCC3-R (5' ACC TTC

ATG GGT GTC TAC CTC CCA). The two fragments were subcloned into the T7/His-tagged pET28 vector (Merck4Biosciences). Subsequently, pET28-NKCC2 and pET28-KCC3 were mutated at codon 45 and 63, respectively, from TAT to TTT to obtain pET28-NKCC2-Y45F and pET28-KCC3-Y63F, using the Quickchange mutagenesis kit (Stratagene, USA).

Previously published constructs used in this study were YFP-SYK (SYK-wt), kinase-dead YFP-SYK-K402R (SYK-kd) and pET-sumo-NBD1 (Mendes et al. 2011). All constructs were verified by automated DNA sequencing. The phosphomimetic and constitutively active SYK-Y352D construct was a gift from Dimitar G. Efremov (ICGEB, Rome, Italy) and provided in pcDNA3-Flag (Carsetti et al. 2009).

2.3. Immunoprecipitation and Western blot procedures

For immunoprecipitation experiments, cells were grown in 60 mm dishes, transfected as described above and lysed on ice in 250 µL lysis buffer (50 mM Tris-HCl pH 7.5, 1% NP-40, 150 mM NaCl, 10% glycerol, 0,1% (m/v) sodium dodecyl sulfate (SDS), 10 mM $MgCl_2$) supplemented with a protease inhibitor cocktail composed of 1 mM PMSF, 1 mM 1,10-phenanthroline, 1 mM EGTA, 10 µM E64, and 10 µg/mL of each aprotinin, leupeptin, and pepstatin A (all from Sigma-Aldrich, Spain). The cell lysates were incubated for 2 h at 4ºC with the specified antibodies (1.5 µg/mL anti-GFP ab1218 (Abcam) or 3 µg/mL anti-Myc clone 9E10 (M5546, Sigma-Aldrich)), then further incubated for 1 h with protein G-agarose beads (Roche), and finally washed three times in cold lysis buffer containing 200 mM NaCl. Proteins were solubilized from the beads in 2x SDS CFTR sample buffer (62.5 mM Tris-HCl pH 6.8, 3% SDS, 10% glycerol, 0.02% bromophenol blue, 196.4 mM dithiothreitol (DTT) and separated in 10% SDS polyacrylamide gels in Protean III mini-gels (BioRad). Gels to assess NKCC2 and KCC3 expression contained 1% glycerol and were run at 4ºC (Mendes et al. 2011).

Following electrophoresis, the separated proteins were transferred onto a PVDF membrane (BioRad) in a cooled Mini Trans-Blot cell (BioRad) at 300 mA, followed by Coomassie Brilliant Blue-staining to check for equal transfer. Membranes were blocked in TBS, 0.1% Triton X-100, 5% milk powder, probed using the indicated antibodies, and then incubated with a secondary peroxidase-conjugated antibody (BioRad) followed by chemiluminescence detection. Primary antibodies used for Western blots

were mouse anti-GFP (11814560001) from Roche, mouse anti-GFP (ab1218), rabbit anti-SYK (ab40781) and rabbit anti-SLC12A6 (ab92951) from Abcam, mouse anti-His (37-2900) from Invitrogen, mouse anti-Flag clone M2 (F3165) and anti-Myc clone 9E10 (M5546) from Sigma-Aldrich, mouse anti-PCNA clone PC10 (NA03) from Calbiochem, and rabbit anti-NKCC2 from Millipore.

2.4 Production of recombinant NKCC2, KCC3 and Sumo-NBD1 and *in vitro* protein kinase assays

For the production of recombinant protein fragments NKCC2$^{12-162}$, KCC3$^{2-135}$, or CFTR-NBD1, the plasmids pET-NKCC2, pET-NKCC2-Y45F, pET-KCC3, pET-KCC3-Y63F and pET-Sumo-NBD1 (Mendes et al. 2011) were expressed in the E. coli BL21 strain upon induction with 0.75 mM isopropylthiogalactosidade (IPTG) and the bacterial pellets harvested at 1400 x g, for 30 min and frozen. For protein extraction, pellets were resuspended in either conventional lysis buffer (50 mM Tris-HCl pH 7.5, 50 mM NaCl, 5 mM $MgCl_2$, 1 mM DTT) for NKCC2, NKCC2-Y45F, KCC3 and KCC3-Y63F, or lysis buffer containing 0.2% (v/v) Tween 20 in case of CFTR-NBD1, in the presence of the protease inhibitor cocktail described above, and then sonicated on ice in 6 cycles of 30 seconds with 10 seconds intervals (Sonics Vibra Cell sonicator, set at 40% power). Following centrifugation of the extracts at 1600x *g*, the supernatant was incubated with Ni-NTA agarose beads (Qiagen, Germany) for 1 h at 4ºC. Beads were washed twice with cold lysis buffer containing 20 mM imidazole and protease inhibitors. Recombinant proteins were eluted and stored in cold lysis buffer containing 250 mM imidazole. Proteins were quantified using the Precision Red Protein Assay Reagent (GL50 from Cytoskeleton) and stored in aliquots at -80ºC.

For *in vitro* protein kinase assay, cells were first lysed under stringent conditions in 250 μl lysis buffer (50 mM Tris-HCl pH 7.5, 150 mM NaCl, 0.5% sodium deoxycholate, 1% NP-40, 0.1% SDS) supplemented with protease inhibitors (see above). Following immunoprecipitation of SYK as described above, the resulting beads were washed three times in cold lysis buffer containing 300 mM NaCl, then resuspended in 20 μl kinase reaction buffer (50 mM Tris-HCl pH 7.5, 10% glycerol, 1 mM DTT, 1 mM Na_3VO_4, 10 mM $MgCl_2$, 100 μM ATP) and incubated at 30ºC for 30 min, in order to reduce background autophosphorylation. Beads containing immunoprecipitated SYK-

wt or SYK-kd were then incubated alone or with the corresponding substrate (200 ng of each recombinant protein) in the presence of 5 μCi γ-[32P] ATP at 30ºC for 30 min. Finally, 2x SDS sample buffer was added, samples boiled and separated by SDS-polyacrylamide gel electrophoresis (PAGE) followed by protein transfer to PVDF membranes and Western blot. Membranes were exposed to X-ray films for 10 min to 72 h and subsequently incubated with the respective antibodies in order to document protein quantities.

2.5 Biotinylation of cell surface proteins

HEK293 cells (either transfected or drug-treated as described above) were washed three times with warm culture medium to remove dead cells, and then placed on ice in a cold room. Cells were washed three times with ice-cold phosphate-buffered saline-CM (PBS-CM) (PBS pH 8.0 containing 0.1mM $CaCl_2$ and 1 mM $MgCl_2$) to ensure arrest of endocytic traffic. Then, cells were incubated for 45 min with 0.5 mg/ml EZ-Link Sulfo-NHS-SS-Biotin (sc-212981, from Santa Cruz Biotechnology) in PBS-CM to label all cell surface proteins. Cells were rinsed twice and incubated for 15 min on ice in ice-cold Tris/Glycine (100 mM Tris-HCl pH 8.0, 150 mM NaCl, 1 mM $MgCl_2$, 0.1 mM $CaCl_2$, 10 mM glycine, 1% BSA) to quench the biotinylation reagent. Cells were again washed three times with cold PBS-CM and lysed in 250 μl pull-down buffer (50 mM Tris-HCl pH 7.5, 100 mM NaCl, 10% glycerol, 1% NP-40) in the presence of the protease inhibitor cocktail (described above). The cell lysates were harvested at 16000 x g at 4ºC for 5 min. An aliquot of 40 μl representing the total protein level was removed and added to 2x SDS CFTR sample buffer (see above), while 200 μl lysate were added to 45 μl streptavidin-agarose beads (Sigma-Aldrich), previously incubated for 1 h in 1 ml cold pull-down buffer containing 2% non-fat milk powder, and washed three times in pull-down buffer. Lysates were incubated with the prepared beads for 1 h at 4ºC, the beads collected by centrifugation of 1 min at 6000 x g, and washed four times in cold wash buffer (100 mM Tris-HCl pH 7.5, 300 mM NaCl, 1% Triton X-100). Captured proteins were recovered in 20 μl of 2x SDS CFTR sample buffer with 100 mM DTT and analyzed by Western blot with specific antibodies, as described above.

2.6 Statistical analysis

Data were analyzed using Student's *t*-tests for paired samples or ANOVA tests followed by post-hoc Tukey's tests when comparing multiple treatments. $P<0.05$ was accepted as the level of statistical significance. Shown data reflect the mean ± SEM from at least three independent experiments.

3. Results

3.1. NKCC2 and KCC3 are a substrate for SYK protein kinase

Recently we described that spleen tyrosine kinase (SYK) can phosphorylate the CFTR chloride channel (Mendes et al. 2011). In particular, we found that the -Y512-D-E-Y motif in the CFTR NBD1 domain was phosphorylated by SYK *in vitro* and that overexpression of SYK in cells inhibited the amount of CFTR present at the cell surface, without affecting total CFTR protein levels.

Because SYK recognizes a well-defined peptide motif, in which the phosphorylated tyrosine is followed by two acidic amino acid residues (Y-E/D-E/D-X), we analyzed the protein sequence of 20 human ion channels or cotransporters involved in sodium, potassium or chloride transport for the presence of this SYK recognition motif (see Table 1). Only two further protein sequences were found to contain the motif: the Na+/K+/2Cl-cotransporter NKCC2 (SLC12A1) at tyrosine 45 and the K+/Cl-cotransporter KCC3 (SLC12A6) at tyrosine 63. Both NKCC2 and KCC3 belong to the solute carrier family 12 (SLC12) of cation-chloride cotransporters and the predicted phosphorylation sites are located in their N-terminal cytoplasmic domains.

We first tested whether SYK could phosphorylate NKCC2 and KCC3 *in vitro*. For this purpose, the N-terminal domains of both cotransporters ($NKCC2^{12-162}$; $KCC3^{2-135}$) were cloned, expressed as recombinant proteins in *E. coli* and purified (Fig. 1A). As a negative control, fragments containing a mutated phosphorylation site were also

expressed, namely NKCC2-Y45 and KCC3-Y63F, in which the predicted target tyrosine was point-mutated to phenylalanine. In parallel, expression vectors encoding wild-type (wt) SYK, its kinase-dead (kd) mutant, or the corresponding empty vector were transfected into HEK293 cells and immunoprecipitated from cells lysed in RIPA buffer in order to minimize the contamination with other co-precipitating kinases from the cell lysate. The SYK-containing beads were washed in protein kinase buffer and then the recombinant substrate proteins (NBD1, NKCC2, NKCC2-Y45F, KCC3, KCC3-Y63F) were added and incubated in the presence of radioactive ATP. As shown in Fig. 1B, we observed that SYK-wt autophosphorylated whereas SYK-kd showed no such activity. Moreover, SYK-wt but not kinase-dead SYK clearly phosphorylated wt NKCC2 and KCC3, confirming the absence of contaminant kinase activities. The NKCC2-Y45F and KCC3-Y63F mutants were poor substrates for SYK-wt.

3.2. SYK activity decreases the expression of NKCC2 at the cell surface

Since SYK phosphorylated NKCC2 *in vitro*, we asked whether SYK would also modulate the expression of NKCC2 at the cell surface, as previously described for CFTR. Thus, HEK293 cells were co-transfected with Myc-tagged NKCC2 and one of the following expression vectors: empty vector, kinase-dead SYK (SYK-kd), or the constitutively active mutant SYK-Y352D (Carsetti et al. 2009). Kinase-dead mutants are commonly employed as dominant negative pathway inhibitors because they can interact with the substrate protein without phosphorylating it, thus blocking the access of the corresponding endogenous kinase. After 24 h the abundance of NKCC2 at the plasma membrane was analyzed by biotinylation of cell surface proteins. As shown in Fig. 2A, the expression of SYK-kd increased over 2-fold the amount of NKCC2 at the cell surface, whereas expression of constitutively active SYK led to a near 2-fold decrease.

Next we tested the effect of downregulating endogenous SYK in HEK293 cells. Cells were transfected with SYK-specific siRNAs (sc-29501 from Santa Cruz Biotechnology), which were able to downregulate SYK expression to approximately 15% of its normal levels (Fig. 2B, grey bars). Under these conditions, we observed a near 6-fold increase for NKCC2 at the cell surface, suggesting again that SYK-mediated phosphorylation of NKCC2 mediates its internalization (Fig. 2B, black bars).

Finally, we used pharmacological inhibitors of SYK kinase activity. HEK293 cells were treated with one of two different SYK inhibitors (BAY 61-3606 and PRT062607) or with the control solvent DMSO for 1 h. Subsequent, analysis of biotinylated surface proteins showed that these inhibitors increased the amount of NKCC2 at the cell surface by 2.5 and 3.5-fold, respectively (Fig. 2C).

In order to demonstrate the effect of SYK inhibition in physiologically more relevant cells, we cultured the mouse *macula densa*-derived cell line (MMDD1). Although we found that these cells clearly expressed endogenous NKCC2 and SYK by Western blot analysis, the biotinylation assay was not able to detect NKCC2 at the surface, even when cells were grown on membrane filters and had formed a polarized cell monolayer (see Suppl. Fig. S1).

3.3. SYK activity increases the expression of KCC3 at the cell surface

In order to compare how SYK activity would modulate the expression of KCC3 at the cell surface, HEK293 cells were co-transfected with Myc-tagged KCC3 and the above-described YFP-tagged expression vectors. When the abundance of KCC3 at the plasma membrane was analyzed by biotinylation of cell surface proteins, the expression of constitutively active SYK was found to upregulate by 2-fold the abundance of KCC3 at the cell surface whereas expression of the SYK-kd protein produced the opposite result (Fig. 3A). Thus, SYK expression appeared to affect KCC3 and NKCC2 in opposite ways.

This effect was further confirmed, as described above for NKCC2, following downregulation of endogenous SYK in HEK293 cells (Fig. 3B) or following cell incubation with pharmacological inhibitors of SYK activity (Fig. 3C). In both cases, a decrease in the KCC3 levels at the cell surface was observed, confirming that SYK exerts opposite effects on NKCC2 and KCC3. A physiologically more relevant cell type is the human proximal tubule-derived cell line (HK-2), however, despite expressing endogenous KCC3 and SYK in total cell lysates, we were not able to detect KCC3 expression at the cell surface (see Suppl. Fig. S1).

3.4 SYK activity modulates the cell surface expression of NKCC2 and KCC3 in opposite ways in the same cell.

As described in the Introduction, previous data indicated that a concerted regulation of NKCC and KCC within the same cell is important for cell volume regulation. In case of NKCC1 and KCC3 it has been well-known that both cotransporters are expressed in the same cell. In order to provide proof-of-principle that the SYK-mediated tyrosine phosphorylation of NKCC2 and KCC3 could convey a concerted regulation within the same cell, we co-transfected HEK293 cells with Myc-NKCC2 and Myc-KCC3, then treated them with SYK inhibitors before determining the amount of biotinylated cell surface levels of both cotransporters. In this experiment, we discriminated between NKCC2 and KCC3 by using antibodies specific for each cotransporter, instead of the anti-Myc antibody. The results are shown in Fig 4A and revealed that two different SYK inhibitors (BAY 61-3606 or PRT062607) were able to increase NKCC2 levels at the cell surface roughly two-fold, while simultaneously decreasing KCC3 levels in the same cell.

3.5 SYK activity contributes to cell-volume regulation.

In order to determine whether the effect of SYK inhibition on cell surface expression (more NKCC2 and less KCC3) would confer a functional advantage to the cell, we challenged co-transfected HEK293 cells by incubating them for 10 min in hypertonic medium. Under these osmotic conditions, cells are known to stimulate NKCC activity to increase ion uptake and compensate the osmotic difference. To investigate these effects, we used a simple semi-quantitative microscopy approach to estimate variations in cell dimension. Phase contrast microscopic images were taken 10 min after exposure to hypertonic medium and the area occupied by individual cells measured using NIH ImageJ software. These analyses revealed that after incubation in hypertonic medium, control cells occupied an area 40% smaller than in isotonic medium, indicating a cell body retraction due to shrinkage (Fig. 4B). In contrast, when co-transfected cells were pre-treated with the SYK inhibitor BAY 61-3606 (i.e. increasing the amount of NKCC2 at the cell surface), they occupied 93% of the area compared to isotonic medium, indicating a more efficient compensation of cell volume (Fig. 4B).

4. Discussion

The results presented in this work identify for the first time that phosphorylation on tyrosine residues modulates the cell surface levels of two key ion cotransporters, NKCC2 and KCC3, involved in regulating electrolyte balance and cell volume.

Besides identifying their phosphorylation sites by protein kinase SYK *in vitro*, we provide evidence that co-expression of a constitutively active SYK into human cells decreased NKCC2 but increased KCC3 cell surface expression, and that the opposite effects were observed upon depletion of endogenous SYK or pharmacological inhibition of its kinase activity. Another major novelty reported here is that the same mechanism can apparently be used by cells to regulate NKCC2 and KCC3 in opposite ways.

The topology of both NKCC2 and KCC3 features a central hydrophobic region with 12 transmembrane spanning domain that is flanked by two cytoplasmic domains: a 180-amino acid N-terminal and a longer 470-amino acid C-terminal domain (Ares et al. 2011). The N-terminal domain of NKCC2 is particularly well studied and harbors important regulatory functions: it includes the SPAK/OSR1 recognition motif $R^{20}FQV$ and contains the ion transport-regulating phosphorylation sites Thr95, 100 and 105 (Rinehart et al. 2009; de los Heros et al. 2014). In this work, we identified another regulatory site in this domain, the SYK-phosphorylated Tyr45 residue.

The SYK-phosphorylatable tyrosine 45 belongs to the first coding exon and locates to the N-terminal cytosolic domain and is thus present in all known NKCC2 splicing variants. The functional properties of NKCC2 are modulated by the generation of at least six alternative splicing variants (Simon et al. 1996; Mount et al. 1999). Three variants derive from inclusion of the mutually exclusive cassette exons 4A, 4B or 4F, which all encode part of transmembrane 2 (TM2) with the adjacent intracellular loop and confer different ion transport kinetics (Castrop and Schnermann 2008). In addition, the terminal NKCC2 exon can give rise to two variants of different length depending on the use of two alternative polyadenylation sites.

Similarly, the KCC3-encoding gene can generate two major splicing variants by inclusion of one of two alternative exons 1: KCC3a encodes 1141 amino acids and contains 59 additional N-terminal residues compared to KCC3b (Mercado et al. 2005); however, both retain the SYK-phosphorylatable tyrosine residue (i.e. Y122 in KCC3a

and Y63 in KCC3b). In case of KCC3, the crucial ion transport-regulatory sites that are phosphorylated by the WNK/SPAK/OSR1 pathway are located in the C-terminal domain. These sites are Thr991 and Thr1048 in KCC3a and are normally phosphorylated in isotonic conditions to inhibit ion transport activity. Curiously, all 4 KCC members share highly homologous sites that are phosphorylated by SPAK/OSR1; however, a tyrosine motif for SYK phosphorylation was only identified in KCC3, indicating a specific control mechanism for this family member. Furthermore, the N-terminal domain of KCC3 contains Ser96 (Ser37 in KCC3b), which is also phosphorylated by SPAK to inhibit ion transport activity (Melo et al. 2013).

Recently, a WNK3-SPAK pathway was proposed to operate on NKCC1 and KCC3 in neuronal cells as the Cl^-/volume-sensitive sensor that prevents cell swelling in response to osmotic stress. For this, a WNK3-dependent activation of SPAK triggers the simultaneous phosphorylation of NKCC1 at Thr203/Thr207/Thr212 and of KCC3 at Thr991 and Thr1048 and this results in stimulation of NKCC1-mediated Cl^- uptake and inhibition of KCC3-mediated Cl^- extrusion (Adragna et al. 2015; Zhang et al. 2016). The importance for cell volume regulation of NKCC and KCC within the same cell had also been shown in pioneering studies using red blood cells (Lytle and McManus 2002).

The phosphorylation by SYK that is described in this manuscript could represent a similar concerted mechanism to regulate simultaneously NKCC2 and KCC3. Indeed, we provided proof-of-principle that such simultaneous regulation occurs when transfected NKCC2 and KCC3 are co-expressed in the same cell (Fig. 4). In addition, SYK inhibition increased the cells' capability to compensate volume changes when exposed to hypertonic conditions. However, it remains to be establish whether cell types exist with simultaneous expression of NKCC2 and KCC3. In the kidney, expression of both cotransporters was assigned to different section of the nephron: NKCC2 in the TAL and KCC3 in the proximal tubule. More recently, however, NKCC2 expression has been reported in colon (Zhu et al. 2011; Xue 2014; Xue and Tang 2016) and brain (Konopacka et al. 2015), tissues that also express KCC3.

With regard to NKCC2, its constitutive targeting to the apical membrane of renal MDCK cells was described to be mediated by a region encompassing amino acids 930 to

1007 in the C-terminal cytosolic domain (Carmosino et al. 2008). Nevertheless, in the TAL only around 5% of total NKCC2 protein were found located in the apical membrane (Ares et al. 2011). Most likely, the maintenance of an intracellular NKCC2 pool represents a mechanism to rapidly increase the cellular ion transport capacity following appropriate stimuli (Mutig 2017), as known in the case of the glucose transporter GLUT4 in response to insulin (Leney and Tavaré 2009). Indeed, upon cAMP stimulation of TAL, cell surface NKCC2 increased rapidly, compatible with release from intracellular storage vesicles (Giménez and Forbush 2003; Ortiz 2006). Mechanistically, the vesicle-associated membrane protein 2 (VAMP2) was found to be involved (Caceres et al. 2014). Concerning KCC3, no such data are available.

Although the experiments described above revealed SYK phosphorylation of NKCC2 or KCC3 as an additional mechanism that can regulate their traffic in HEK293 cells, it was not possible to validate the effect in the available physiologically relevant cell lines from the TAL or proximal tubule. Nevertheless, our findings have several potential biomedical implications. First, NKCC2 in the kidney represents the major target for diuretic drugs, the so-called loop diuretics such as furosemide, which are widely used in the treatment of hypertension. By decreasing the amount of sodium retained in the TAL, the plasma volume is reduced and helps to counteract high blood pressure. In this sense, modulating the SYK-mediated tyrosine phosphorylation of NKKC2 may represent an alternative pharmacologic target to treat hypertension, which does not rely on the inhibition of the ion transport activity but rather on the amount of NKCC2 present at the cell surface. Although the protein kinase activity of SYK itself is a potential candidate, the widespread role of SYK signaling in immune cells (Mócsai et al. 2010) may lead to undesirable side effects. It will be interesting to determine what other cellular proteins are involved downstream of the phosphorylation event so that more specific drug targets can be identified.

Second, the sequence context around the phosphorylated NKCC2 Tyr 63 could be involved in the variation of blood pressure found in the normal population, given that *SLC12A1* was identified as a modifier gene during the genetic analysis of samples from the Framingham Heart Study, a defined population study over 35 years. Some genetic variants are protective against hypertension (Ji et al. 2008; Acuña et al. 2011; Welling 2014) because they decrease renal ion resorption. This may be caused by variants affecting NKCC2 biosynthesis, membrane trafficking, ion transport, or

regulation, possibly including the tyrosine phosphorylation described in this manuscript.

Third, KCC3-mediated cell volume regulation is important for the normal development and functioning of peripheral nerves (Byun and Delpire 2007). In KCC3$^{-/-}$ mice, periaxonal swelling as a sign of a blocked efflux pathway was reported and followed by neurodegeneration. In humans, the corresponding autosomal recessive agenesis of the corpus callosum with peripheral neuropathy (ACCPN), also known as Andermann syndrome, is caused by truncating mutations in the KCC3-encoding SCL12A6 gene, or by missense mutations leading to defective regulation of its ion transport activity (Kahle et al. 2016). Although the WNK/SPAK-mediated phosphorylation of KCC3 at Thr1098 seems to be the major mechanism in the cellular response to acute cell volume changes, the contribution of the amount of KCC3 present at the cell surface remains to be clarified. Myelin and axonal disorders have a wide spectrum of underlying etiologies but are common to a large group of human neurological diseases (Byun and Delpire 2007) and may benefit from knowledge on KCC3 regulation.

Finally, various ion channels and cotransporters promote crucial cellular functions during tumor progression, based on their roles in cell volume regulation, membrane potential and interaction at the cell surface with receptors or other membrane proteins (Kunzelmann 2005; Schönherr 2005). Accordingly, changes in expression or regulation of KCC3 have been observed in primary tumors, such as from brain, cervix, breast, ovary or esophagus (Shen et al. 2004; Hsu et al. 2007b, a; Gagnon 2012; Kitagawa et al. 2013; Shiozaki et al. 2014; Chiu et al. 2014). Any upregulation of K^+/Cl^- cotransport activity was found to benefit cancer cells in their growth or invasiveness related to epithelial mesenchymal transition (Shen et al. 2001; Chen et al. 2010; Salin-Cantegrel et al. 2013). Thus, knowledge of the mechanisms regulating the cell surface abundance of KCC3, such as the tyrosine phosphorylation described here, may be important for patient stratification or therapeutic options in certain tumor subtypes.

In conclusion, we found that the ion cotransporters NKCC2 and KCC3 are phosphorylated on an N-terminal tyrosine residue by protein kinase SYK and that experimental manipulation either of SYK expression levels or of its catalytic activity affect the cell surface abundance of these cotransporters. Interestingly, the very same

phosphorylation pathway leads to a decrease in NKCC2 but to an increase in KCC3 surface levels.

Acknowledgements

This work was supported by Fundação para a Ciência e Tecnologia (FCT) [grants PTDC/SAU-ORG/119782/2010 and PTDC/BIA-CEL/28408/2017 to PJ, grant UID/MULTI/04046/2019 to the research unit BioISI, and fellowship SFRH/BD/52488/2014 from the BioSYS PhD programme PD65-2012 to CAL]. The authors acknowledge the following colleagues for providing reagents used in this study: K. Mutig, Charité, Berlin, Germany; Maria J. Valente, REQUIMTE, Porto, Portugal; Dimitar G. Efremov, ICGEB, Rome, Italy.

Competing interest statement

The authors have no competing interests to declare.

References

Acuña R, Martínez-de-la-Maza L, Ponce-Coria J, et al (2011) Rare mutations in SLC12A1 and SLC12A3 protect against hypertension by reducing the activity of renal salt cotransporters: J Hypertens 29:475–483. doi: 10.1097/HJH.0b013e328341d0fd

Adragna NC, Ravilla NB, Lauf PK, et al (2015) Regulated phosphorylation of the K-Cl cotransporter KCC3 is a molecular switch of intracellular potassium content and cell volume homeostasis. Front Cell Neurosci 9:255. doi: 10.3389/fncel.2015.00255

Ares GR, Caceres PS, Ortiz PA (2011) Molecular regulation of NKCC2 in the thick ascending limb. Am J Physiol-Ren Physiol 301:F1143–F1159. doi: 10.1152/ajprenal.00396.2011

Arroyo JP, Kahle KT, Gamba G (2013) The SLC12 family of electroneutral cation-coupled chloride cotransporters. Mol Aspects Med 34:288–298. doi: 10.1016/j.mam.2012.05.002

Byun N, Delpire E (2007) Axonal and periaxonal swelling precede peripheral neurodegeneration in KCC3 knockout mice. Neurobiol Dis 28:39–51. doi: 10.1016/j.nbd.2007.06.014

Caceres PS, Ares GR, Ortiz PA (2009) cAMP Stimulates Apical Exocytosis of the Renal Na^+-K^+-$2Cl^-$ Cotransporter NKCC2 in the Thick Ascending Limb: ROLE OF PROTEIN KINASE A. J Biol Chem 284:24965–24971. doi: 10.1074/jbc.M109.037135

Caceres PS, Mendez M, Ortiz PA (2014) Vesicle-associated Membrane Protein 2 (VAMP2) but Not VAMP3 Mediates cAMP-stimulated Trafficking of the Renal Na^+-K^+-$2Cl^-$ Co-transporter NKCC2 in Thick Ascending Limbs. J Biol Chem 289:23951–23962. doi: 10.1074/jbc.M114.589333

Carmosino M, Giménez I, Caplan M, Forbush B (2008) Exon loss accounts for differential sorting of Na-K-Cl cotransporters in polarized epithelial cells. Mol Biol Cell 19:4341–4351. doi: 10.1091/mbc.e08-05-0478

Carsetti L, Laurenti L, Gobessi S, et al (2009) Phosphorylation of the activation loop tyrosines is required for sustained Syk signaling and growth factor-independent B-cell proliferation. Cell Signal 21:1187–1194. doi: 10.1016/j.cellsig.2009.03.007

Castaneda-Bueno M, Cervantes-Perez LG, Vazquez N, et al (2012) Activation of the renal Na+:Cl- cotransporter by angiotensin II is a WNK4-dependent process. Proc Natl Acad Sci 109:7929–7934. doi: 10.1073/pnas.1200947109

Castrop H, Schießl IM (2014) Physiology and pathophysiology of the renal Na-K-2Cl cotransporter (NKCC2). Am J Physiol-Ren Physiol 307:F991–F1002. doi: 10.1152/ajprenal.00432.2014

Castrop H, Schnermann J (2008) Isoforms of renal Na-K-2Cl cotransporter NKCC2: expression and functional significance. Am J Physiol-Ren Physiol 295:F859–F866. doi: 10.1152/ajprenal.00106.2008

Chen Y-F, Chou C-Y, Ellory JC, Shen M-R (2010) The emerging role of KCl cotransport in tumor biology. Am J Transl Res 2:345–355

Chiu M-H, Liu H-S, Wu Y-H, et al (2014) SPAK mediates KCC3-enhanced cervical cancer tumorigenesis. FEBS J 281:2353–2365. doi: 10.1111/febs.12787

de los Heros P, Alessi DR, Gourlay R, et al (2014) The WNK-regulated SPAK/OSR1 kinases directly phosphorylate and inhibit the K^+–Cl^- co-transporters. Biochem J 458:559–573. doi: 10.1042/BJ20131478

Esteva-Font C, Ballarin J, Fernández-Llama P (2012) Molecular biology of water and salt regulation in the kidney. Cell Mol Life Sci 69:683–695. doi: 10.1007/s00018-011-0858-4

Gagnon KB (2012) High-grade Glioma Motility Reduced by Genetic Knockdown of KCC3. Cell Physiol Biochem 30:466–476. doi: 10.1159/000339040

Gamba G, Friedman PA (2009) Thick ascending limb: the Na+:K+:2Cl− co-transporter, NKCC2, and the calcium-sensing receptor, CaSR. Pflüg Arch - Eur J Physiol 458:61–76. doi: 10.1007/s00424-008-0607-1

Giménez I, Forbush B (2003) Short-term Stimulation of the Renal Na-K-Cl Cotransporter (NKCC2) by Vasopressin Involves Phosphorylation and Membrane Translocation of the Protein. J Biol Chem 278:26946–26951. doi: 10.1074/jbc.M303435200

Gunaratne R, Braucht DWW, Rinschen MM, et al (2010) Quantitative phosphoproteomic analysis reveals cAMP/vasopressin-dependent signaling pathways in native renal thick ascending limb cells. Proc Natl Acad Sci 107:15653–15658. doi: 10.1073/pnas.1007424107

Howard HC, Mount DB, Rochefort D, et al (2002) The K-Cl cotransporter KCC3 is mutant in a severe peripheral neuropathy associated with agenesis of the corpus callosum. Nat Genet 32:384–392. doi: 10.1038/ng1002

Hsu Y-M, Chen Y-F, Chou C-Y, et al (2007a) KCl Cotransporter-3 Down-regulates E-Cadherin/β-Catenin Complex to Promote Epithelial-Mesenchymal Transition. Cancer Res 67:11064–11073. doi: 10.1158/0008-5472.CAN-07-2443

Hsu Y-M, Chou C-Y, Chen HHW, et al (2007b) IGF-1 upregulates electroneutral K-Cl cotransporter KCC3 and KCC4 which are differentially required for breast cancer cell proliferation and invasiveness. J Cell Physiol 210:626–636. doi: 10.1002/jcp.20859

Ji W, Foo JN, O'Roak BJ, et al (2008) Rare independent mutations in renal salt handling genes contribute to blood pressure variation. Nat Genet 40:592–599. doi: 10.1038/ng.118

Kahle KT, Flores B, Bharucha-Goebel D, et al (2016) Peripheral motor neuropathy is associated with defective kinase regulation of the KCC3 cotransporter. Sci Signal 9:ra77–ra77. doi: 10.1126/scisignal.aae0546

Kahle KT, Khanna AR, Alper SL, et al (2015) K-Cl cotransporters, cell volume homeostasis, and neurological disease. Trends Mol Med 21:513–523. doi: 10.1016/j.molmed.2015.05.008

Kahle KT, Rinehart J, Ring A, et al (2006) WNK protein kinases modulate cellular Cl- flux by altering the phosphorylation state of the Na-K-Cl and K-Cl cotransporters. Physiology 21:326–335. doi: 10.1152/physiol.00015.2006

Kim GH, Ecelbarger CA, Mitchell C, et al (1999) Vasopressin increases Na-K-2Cl cotransporter expression in thick ascending limb of Henle's loop. Am J Physiol 276:F96–F103. doi: 10.1152/ajprenal.1999.276.1.F96

Kitagawa M, Niisato N, Shiozaki A, et al (2013) A regulatory role of K+–Cl− cotransporter in the cell cycle progression of breast cancer MDA-MB-231 cells. Arch Biochem Biophys 539:92–98. doi: 10.1016/j.abb.2013.06.014

Kleta R, Bockenhauer D (2006) Bartter Syndromes and Other Salt-Losing Tubulopathies. Nephron Physiol 104:p73–p80. doi: 10.1159/000094001

Konopacka A, Qiu J, Yao ST, et al (2015) Osmoregulation Requires Brain Expression of the Renal Na-K-2Cl Cotransporter NKCC2. J Neurosci 35:5144–5155. doi: 10.1523/JNEUROSCI.4121-14.2015

Kunzelmann K (2005) Ion Channels and Cancer. J Membr Biol 205:159–173. doi: 10.1007/s00232-005-0781-4

Leney SE, Tavaré JM (2009) The molecular basis of insulin-stimulated glucose uptake: signalling, trafficking and potential drug targets. J Endocrinol 203:1–18. doi: 10.1677/JOE-09-0037

Leto D, Saltiel AR (2012) Regulation of glucose transport by insulin: traffic control of GLUT4. Nat Rev Mol Cell Biol 13:383–396. doi: 10.1038/nrm3351

Lytle C, McManus T (2002) Coordinate modulation of Na-K-2Cl cotransport and K-Cl cotransport by cell volume and chloride. Am J Physiol-Cell Physiol 283:C1422–C1431. doi: 10.1152/ajpcell.00130.2002

Matos AM, Gomes-Duarte A, Faria M, et al (2018) Prolonged co-treatment with HGF sustains epithelial integrity and improves pharmacological rescue of Phe508del-CFTR. Sci Rep 8: 13026. doi: 10.1038/s41598-018-31514-2

McCormick JA, Yang C-L, Ellison DH (2008) WNK Kinases and Renal Sodium Transport in Health and Disease: An Integrated View. Hypertension 51:588–596. doi: 10.1161/HYPERTENSIONAHA.107.103788

Melo Z, de los Heros P, Cruz-Rangel S, et al (2013) N-terminal Serine Dephosphorylation Is Required for KCC3 Cotransporter Full Activation by Cell Swelling. J Biol Chem 288:31468–31476. doi: 10.1074/jbc.M113.475574

Mendes AI, Matos P, Moniz S, et al (2011) Antagonistic regulation of cystic fibrosis transmembrane conductance regulator cell surface expression by protein kinases WNK4 and spleen tyrosine kinase. Mol Cell Biol 31:4076–4086. doi: 10.1128/MCB.05152-11

Mercado A, Vázquez N, Song L, et al (2005) NH_2-terminal heterogeneity in the KCC3 K^+-Cl^- cotransporter. Am J Physiol-Ren Physiol 289:F1246–F1261. doi: 10.1152/ajprenal.00464.2004

Mócsai A, Ruland J, Tybulewicz VLJ (2010) The SYK tyrosine kinase: a crucial player in diverse biological functions. Nat Rev Immunol 10:387–402. doi: 10.1038/nri2765

Moes AD, van der Lubbe N, Zietse R, et al (2014) The sodium chloride cotransporter SLC12A3: new roles in sodium, potassium, and blood pressure regulation. Pflüg Arch - Eur J Physiol 466:107–118. doi: 10.1007/s00424-013-1407-9

Mount DB, Baekgaard A, Hall AE, et al (1999) Isoforms of the Na-K-2Cl cotransporter in murine TAL I. Molecular characterization and intrarenal localization. Am J Physiol 276:F347-358. doi: 10.1152/ajprenal.1999.276.3.F347

Mutig K (2017) Trafficking and regulation of the NKCC2 cotransporter in the thick ascending limb: Curr Opin Nephrol Hypertens 26:392–397. doi: 10.1097/MNH.0000000000000351

Ortiz PA (2006) cAMP increases surface expression of NKCC2 in rat thick ascending limbs: role of VAMP. Am J Physiol Renal Physiol 290:F608-616. doi: 10.1152/ajprenal.00248.2005

Pedersen SF, Hoffmann EK, Novak I (2013) Cell volume regulation in epithelial physiology and cancer. Front Physiol 4:233. doi: 10.3389/fphys.2013.00233

Piala AT, Moon TM, Akella R, et al (2014) Chloride Sensing by WNK1 Involves Inhibition of Autophosphorylation. Sci Signal 7:ra41–ra41. doi: 10.1126/scisignal.2005050

Piechotta K, Lu J, Delpire E (2002) Cation Chloride Cotransporters Interact with the Stress-related Kinases Ste20-related Proline-Alanine-rich Kinase (SPAK) and Oxidative Stress Response 1 (OSR1). J Biol Chem 277:50812–50819. doi: 10.1074/jbc.M208108200

Richardson C, Sakamoto K, de los Heros P, et al (2011) Regulation of the NKCC2 ion cotransporter by SPAK-OSR1-dependent and -independent pathways. J Cell Sci 124:789–800. doi: 10.1242/jcs.077230

Rinehart J, Maksimova YD, Tanis JE, et al (2009) Sites of Regulated Phosphorylation that Control K-Cl Cotransporter Activity. Cell 138:525–536. doi: 10.1016/j.cell.2009.05.031

Salin-Cantegrel A, Shekarabi M, Rasheed S, et al (2013) Potassium-Chloride Cotransporter 3 Interacts with Vav2 to Synchronize the Cell Volume Decrease Response with Cell Protrusion Dynamics. PLoS ONE 8:e65294. doi: 10.1371/journal.pone.0065294

Saritas T, Borschewski A, McCormick JA, et al (2013) SPAK Differentially Mediates Vasopressin Effects on Sodium Cotransporters. J Am Soc Nephrol 24:407–418. doi: 10.1681/ASN.2012040404

Schönherr R (2005) Clinical Relevance of Ion Channels for Diagnosis and Therapy of Cancer. J Membr Biol 205:175–184. doi: 10.1007/s00232-005-0782-3

Shen M-R, Chou C-Y, Hsu K-F, et al (2001) The KCl cotransporter isoform KCC3 can play an important role in cell growth regulation. Proc Natl Acad Sci 98:14714–14719. doi: 10.1073/pnas.251388798

Shen M-R, Lin A-C, Hsu Y-M, et al (2004) Insulin-like Growth Factor 1 Stimulates KCl Cotransport, Which Is Necessary for Invasion and Proliferation of Cervical Cancer and Ovarian Cancer Cells. J Biol Chem 279:40017–40025. doi: 10.1074/jbc.M406706200

Shiozaki A, Takemoto K, Ichikawa D, et al (2014) The K–Cl Cotransporter KCC3 as an Independent Prognostic Factor in Human Esophageal Squamous Cell Carcinoma. BioMed Res Int 2014:1–12. doi: 10.1155/2014/936401

Simon DB, Karet FE, Hamdan JM, et al (1996) Bartter's syndrome, hypokalaemic alkalosis with hypercalciuria, is caused by mutations in the Na–K–2CI cotransporter NKCC2. Nat Genet 13:183–188. doi: 10.1038/ng0696-183

Terker AS, Zhang C, Erspamer KJ, et al (2016) Unique chloride-sensing properties of WNK4 permit the distal nephron to modulate potassium homeostasis. Kidney Int 89:127–134. doi: 10.1038/ki.2015.289

Veríssimo F, Jordan P (2001) WNK kinases, a novel protein kinase subfamily in multi-cellular organisms. Oncogene 20:5562–5569. doi: 10.1038/sj.onc.1204726

Vitari AC, Deak M, Morrice NA, Alessi DR (2005) The WNK1 and WNK4 protein kinases that are mutated in Gordon's hypertension syndrome phosphorylate and activate SPAK and OSR1 protein kinases. Biochem J 391:17–24. doi: 10.1042/BJ20051180

Vitari AC, Thastrup J, Rafiqi FH, et al (2006) Functional interactions of the SPAK/OSR1 kinases with their upstream activator WNK1 and downstream substrate NKCC1. Biochem J 397:223–231. doi: 10.1042/BJ20060220

Watanabe M, Fukuda A (2015) Development and regulation of chloride homeostasis in the central nervous system. Front Cell Neurosci 9:371. doi: 10.3389/fncel.2015.00371

Welker P, Böhlick A, Mutig K, et al (2008) Renal Na+-K+-Cl- cotransporter activity and vasopressin-induced trafficking are lipid raft-dependent. Am J Physiol Renal Physiol 295:F789-802. doi: 10.1152/ajprenal.90227.2008

Welling PA (2014) Rare mutations in renal sodium and potassium transporter genes exhibit impaired transport function: Curr Opin Nephrol Hypertens 23:1–8. doi: 10.1097/01.mnh.0000437204.84826.99

Xue H (2014) Localization and vasopressin regulation of the Na^+-K^+-$2Cl^-$ cotransporter in the distal colonic epithelium. World J Gastroenterol 20:4692. doi: 10.3748/wjg.v20.i16.4692

Xue H, Tang X (2016) Effect of vasopressin on Na+–K+–2Cl− cotransporter (NKCC) and the signaling mechanisms on the murine late distal colon. Eur J Pharmacol 771:241–246. doi: 10.1016/j.ejphar.2015.11.051

Zagórska A, Pozo-Guisado E, Boudeau J, et al (2007) Regulation of activity and localization of the WNK1 protein kinase by hyperosmotic stress. J Cell Biol 176:89–100. doi: 10.1083/jcb.200605093

Zhang J, Gao G, Begum G, et al (2016) Functional kinomics establishes a critical node of volume-sensitive cation-Cl− cotransporter regulation in the mammalian brain. Sci Rep 6: 35986. doi: 10.1038/srep35986

Zhu J-X, Xue H, Ji T, Xing Y (2011) Cellular localization of NKCC2 and its possible role in the Cl− absorption in the rat and human distal colonic epithelia. Transl Res 158:146–154. doi: 10.1016/j.trsl.2011.04.003

Legends to Tables and Figures

Table 1. List of 20 human ion channels or cotransporters involved in sodium, potassium or chloride transport that were inspected for the presence of the peptide motif Y-E/D-E/D-X recognized and phosphorylated by SYK.

Fig. 1. Protein kinase SYK phosphorylates NKCC2 and KCC3 *in vitro*.

(A) The N-terminal domains of NKCC2 (amino acids 12-162) and KCC3 (amino acids 2-135), as well as their phosphorylation site mutants containing phenylalanine instead of the predicted target tyrosine, were affinity-purified from lysed *E. coli*. Shown are Coomassie-stained polyacrylamide gels after electrophoretic separation of proteins from the indicated fractions: P- insoluble pellet after lysis; S- soluble lysate fraction, subsequent eluates E1-E3 from the Ni-NTA affinity column; M- molecular weight marker of 25 kDa.

(B) Wild-type (wt) SYK or its kinase-dead (kd) mutant were immunoprecipitated from transfected HEK293 cells and incubated in protein kinase buffer in the presence of radioactive ATP with the indicated recombinant substrate proteins (NBD1, NKCC2, NKCC2-Y45F, KCC3, KCC3-Y63F). Proteins were separated by SDS-PAGE and transferred to PVDF membrane. Top panel shows the radioactive proteins detected by exposing the membrane to x-ray films (Kinase Assay) and bottom panel the corresponding immunodetection (WB) to document the amounts of the indicated recombinant or immunoprecipitated proteins in the assay. Note that SYK-wt (but not SYK-kd) phosphorylated itself as well as NKCC2 and KCC3, whereas the mutants NKCC2-Y45F and KCC3-Y63F were poor substrates. NBD1 served as a previously described control (Mendes et al. 2011). As a negative control for the immunoprecipitation, lysates from cells transfected with an empty yellow-fluorescence protein vector (YFP-EV) were used.

Fig. 2. Experimental manipulation of either SYK expression levels or its catalytic activity modulates the levels of NKCC2 at the plasma membrane of HEK293 cells.

(A) Effect of overexpression of SYK mutants. Cells were co-transfected with Myc-tagged NKCC2 and one of the following expression vectors: empty vector (EV), kinase-dead YFP-tagged mutant SYK-kd, or constitutively active Flag-tagged mutant SYK-Y352D. Data represent means ± SEM. Statistical analysis with ANOVA ($p<0.02$) followed by Tukey's test (* = $p < 0.05$).

(B) Effect of depleting endogenous SYK expression. Cells were co-transfected with Myc-tagged NKCC2 and either a control (siLUC) or a SYK-specific (siSYK) siRNA. Note the successful downregulation of SYK expression. Data represent means ± SEM; * = $p < 0.01$ by T-test.

(C) Effect of inhibition of SYK catalytic activity. Cells were transfected with Myc-tagged NKCC2 and 24 h later treated for 1 h with control solvent DMSO, or with SYK inhibitors BAY 61-3606 or PRT062607. Data represent means ± SEM. Statistical analysis with ANOVA ($p<0.001$) followed by Tukey's test (* = $p < 0.05$).

(A-C) After the treatments described above, cell surface proteins were biotinylated, cells then lysed and proteins resolved by SDS-PAGE and Western blot. Left panel: Detection of the indicated proteins in whole cell lysates (WCL) or in the biotinylated protein fraction (surface). The proliferating cell nuclear antigen protein (PCNA) served as a loading and contamination control, respectively. Lysates from cells incubated without the biotinylation reagent (w/o biotin) served as additional negative control. Right panel: corresponding quantification of NKCC2 detection in the biotinylated cell surface fraction, obtained from at least three independent experiments.

Fig. 3. Experimental manipulation of either SYK expression levels or its catalytic activity modulates the levels of KCC3 at the plasma membrane of HEK293 cells. Cells were transfected with Myc-tagged KCC3 and then treated and analyzed as described in the legend to Fig. 2. (A) Effect of overexpression of SYK mutants. Statistical analysis with ANOVA ($p<0.002$) followed by Tukey's test (* = $p < 0.05$). (B) Effect of depleting endogenous SYK expression; * = $p < 0.05$ by T-test. (C) Effect of inhibition of SYK

catalytic activity. Statistical analysis with ANOVA ($p<0.005$) followed by Tukey's test (* = $p < 0.01$).

Fig.4. SYK activity contributes to cell volume regulation.

(A) Inhibition of endogenous SYK activity modulates the cell surface expression of NKCC2 and KCC3 in opposite ways in the same cell. HEK293 cells were co-transfected with Myc-tagged KCC3 and NKCC2, then treated and analyzed as described in the legend to Fig. 2. Note that NKCC2 or KCC3 were distinguished in whole cell lysates (WCL) or in the biotinylated protein fraction (surface) by using specific primary antibodies. Lower panel: corresponding quantification of NKCC2 and KCC3 detection in the biotinylated cell surface fraction, obtained from at least five independent experiments. Statistical analysis with ANOVA ($p<0.01$ for NKCC2, and $p<0.001$ for KCC3 data) followed by Tukey's test (* = $p < 0.05$; ** = $p < 0.01$).

(B) Inhibition of endogenous SYK activity contributes to cell-volume regulation. HEK293 cells were co-transfected with Myc-tagged KCC3 and NKCC2, then treated for 1 h with control solvent DMSO, or with SYK inhibitor BAY 61-3606. Phase contrast microscopy images (600 x) were digitally recorded in isotonic medium, then cells were transferred to hypertonic for 10 min and the same cells imaged again. The area covered by cells was measured in the digitally recorded images, and differences obtained from three independent experiments were graphically displayed (lower panel). Data represent means ± SEM; * = $p < 0.05$ by T-test.

Figure 1

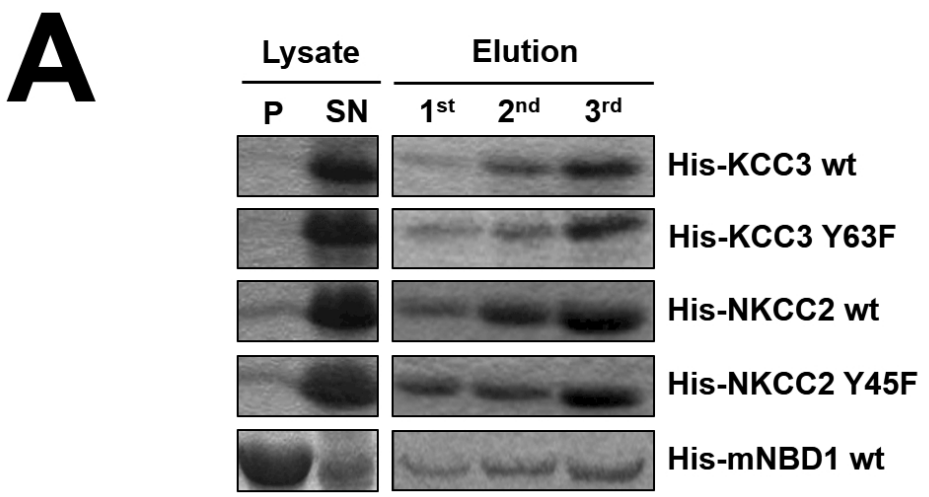
A
Lysate
Elution
P
SN
1st
2nd
3rd
His-KCC3 wt
His-KCC3 Y63F
His-NKCC2 wt
His-NKCC2 Y45F
His-mNBD1 wt

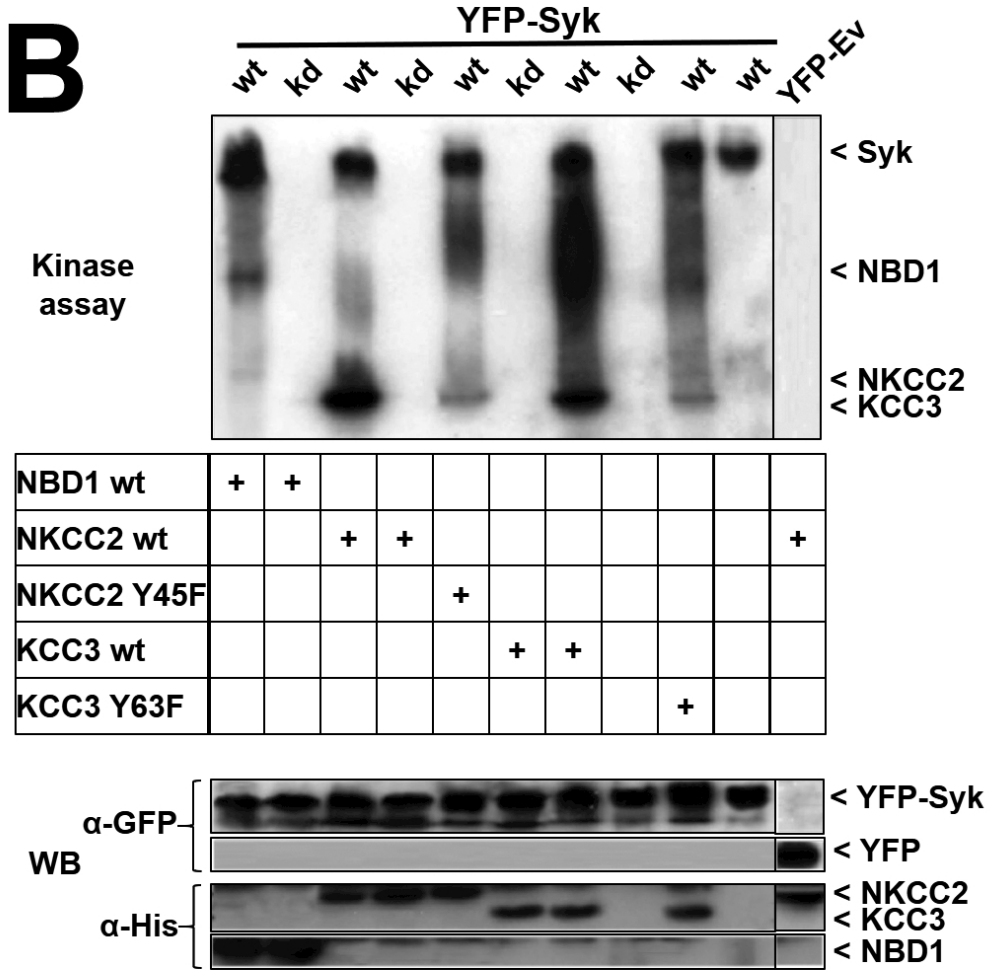
B
YFP-Syk
wt
kd
wt
kd
wt
kd
wt
kd
wt
wt
YFP-Ev
Kinase assay
< Syk
< NBD1
< NKCC2
< KCC3
NBD1 wt
NKCC2 wt
NKCC2 Y45F
KCC3 wt
KCC3 Y63F
α-GFP
WB
α-His
< YFP-Syk
< YFP
< NKCC2
< KCC3
< NBD1

Figure 2

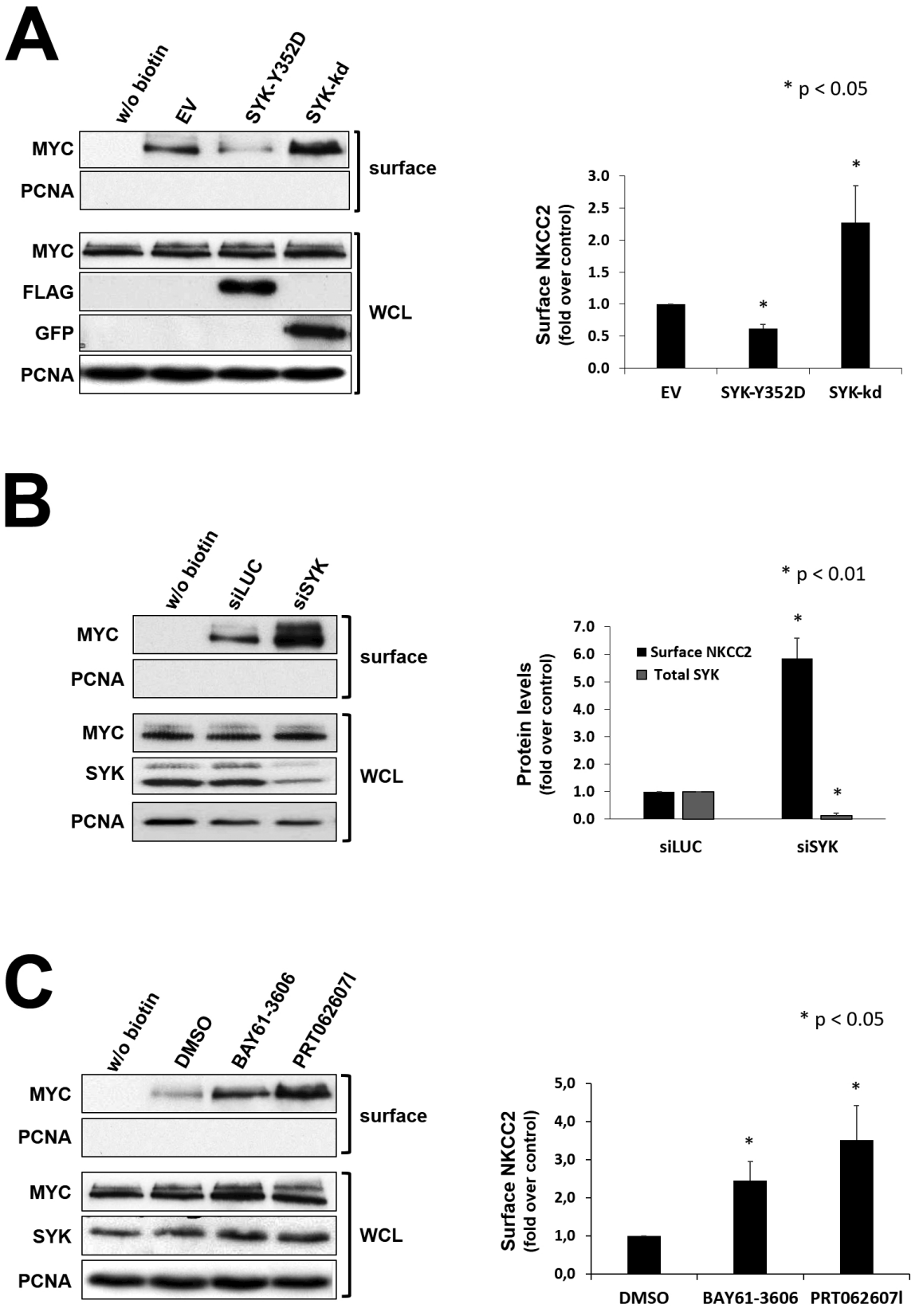
A
w/o biotin
EV
SYK-Y352D
SYK-kd
MYC
PCNA
surface
MYC
FLAG
GFP
PCNA
WCL
* p < 0.05
Surface NKCC2 (fold over control)
3.0
2.5
2.0
1.5
1.0
0.5
0.0
EV
SYK-Y352D
SYK-kd
B
w/o biotin
siLUC
siSYK
MYC
PCNA
surface
MYC
SYK
PCNA
WCL
* p < 0.01
Protein levels (fold over control)
Surface NKCC2
Total SYK
7.0
6.0
5.0
4.0
3.0
2.0
1.0
0.0
siLUC
siSYK
C
w/o biotin
DMSO
BAY61-3606
PRT062607l
MYC
PCNA
surface
MYC
SYK
PCNA
WCL
* p < 0.05
Surface NKCC2 (fold over control)
5,0
4,0
3,0
2,0
1,0
0,0
DMSO
BAY61-3606
PRT062607l

Figure 3

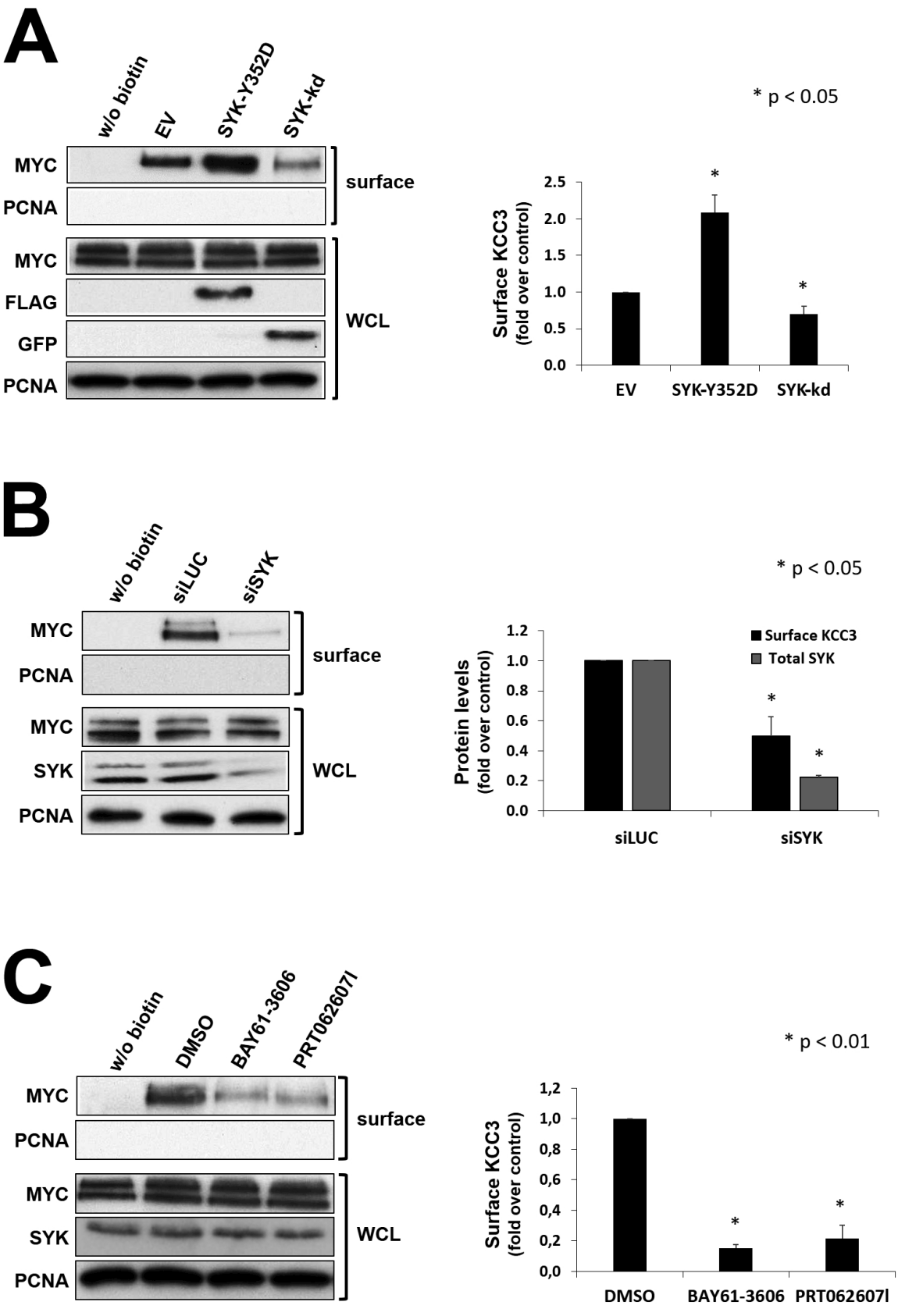
A
w/o biotin
EV
SYK-Y352D
SYK-kd
MYC
PCNA
surface
MYC
FLAG
GFP
PCNA
WCL
* p < 0.05
Surface KCC3
(fold over control)
2.5
2.0
1.5
1.0
0.5
0.0
EV
SYK-Y352D
SYK-kd
B
w/o biotin
siLUC
siSYK
MYC
PCNA
surface
MYC
SYK
PCNA
WCL
* p < 0.05
Protein levels
(fold over control)
1.2
1.0
0.8
0.6
0.4
0.2
0.0
Surface KCC3
Total SYK
siLUC
siSYK
C
w/o biotin
DMSO
BAY61-3606
PRT062607l
MYC
PCNA
surface
MYC
SYK
PCNA
WCL
* p < 0.01
Surface KCC3
(fold over control)
1,2
1,0
0,8
0,6
0,4
0,2
0,0
DMSO
BAY61-3606
PRT062607l

Figure 4

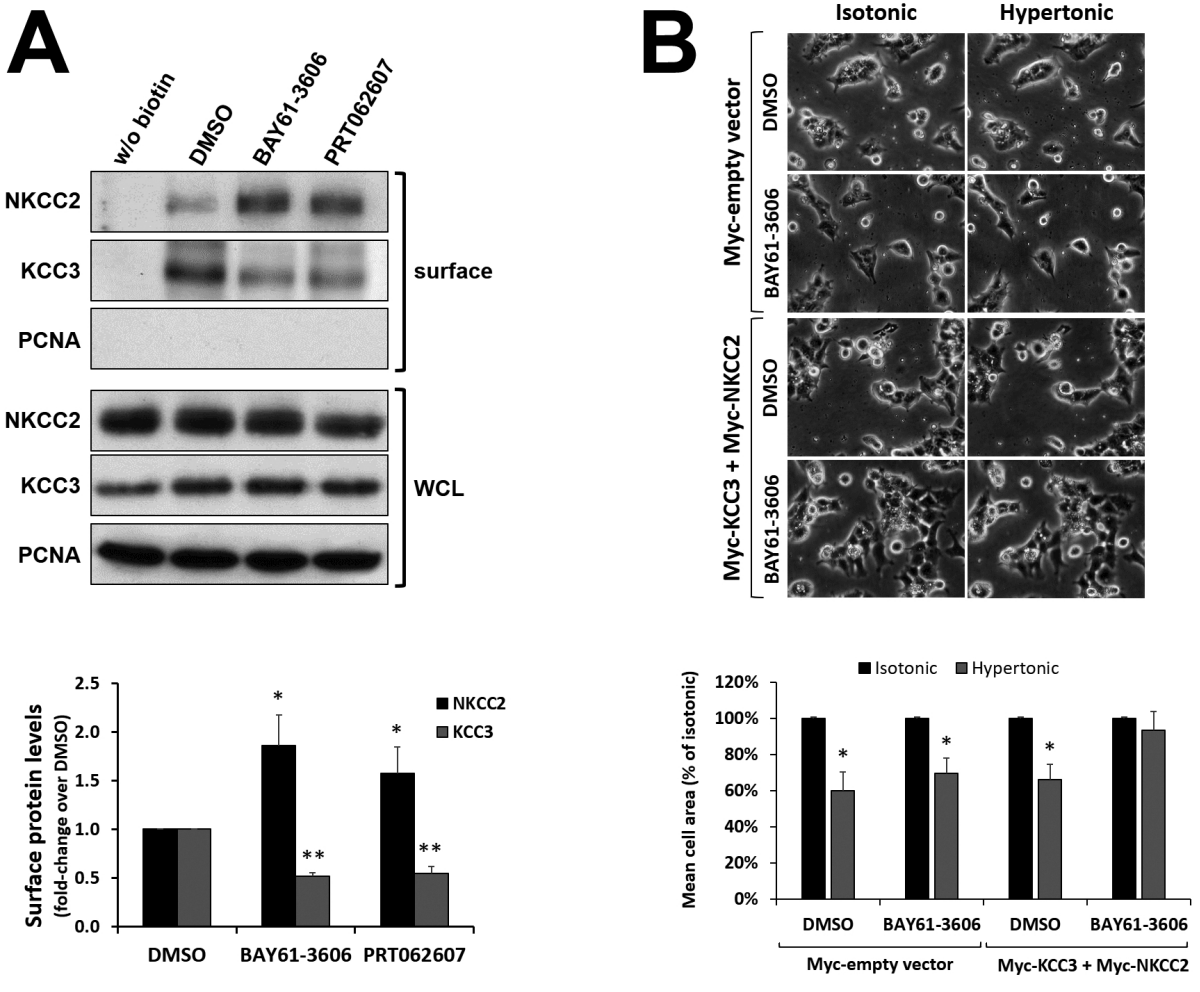
A
w/o biotin
DMSO
BAY61-3606
PRT062607
NKCC2
KCC3
PCNA
surface
NKCC2
KCC3
PCNA
WCL
Surface protein levels
(fold-change over DMSO)
NKCC2
KCC3
DMSO
BAY61-3606
PRT062607
B
Isotonic
Hypertonic
Myc-empty vector
DMSO
BAY61-3606
Myc-KCC3 + Myc-NKCC2
DMSO
BAY61-3606
Mean cell area (% of isotonic)
Isotonic
Hypertonic
DMSO
BAY61-3606
DMSO
BAY61-3606
Myc-empty vector
Myc-KCC3 + Myc-NKCC2

Supplementary Material

to manuscript

Tyrosine phosphorylation modulates cell surface expression of chloride cotransporters NKCC2 and KCC3

Cláudia Almeida Loureiro, Patrícia Barros, Paulo Matos, Peter Jordan

Fig. S1. Expression of endogenous SYK, NKCC2 and KCC3 proteins in physiologically relevant cells types. (**A**) Mouse *macula densa*-derived cells (MMDD1) or (**B**) human proximal tubule HK-2 cells were grown on collagen-coated filter inserts (as described under Materials and methods), then cell surface proteins were biotinylated, cells lysed and proteins resolved by SDS-PAGE and Western blot for the detection of the indicated proteins in whole cell lysates (WCL) or in the biotinylated protein fraction (surface). The PCNA protein served as a loading and contamination control, respectively. (**C**) Detection of endogenous SYK protein expression in whole cell lysates of mouse MMDD1 and human HK-2 cells. Note that antibody affinity may not be comparable due to the species difference of both lysates.

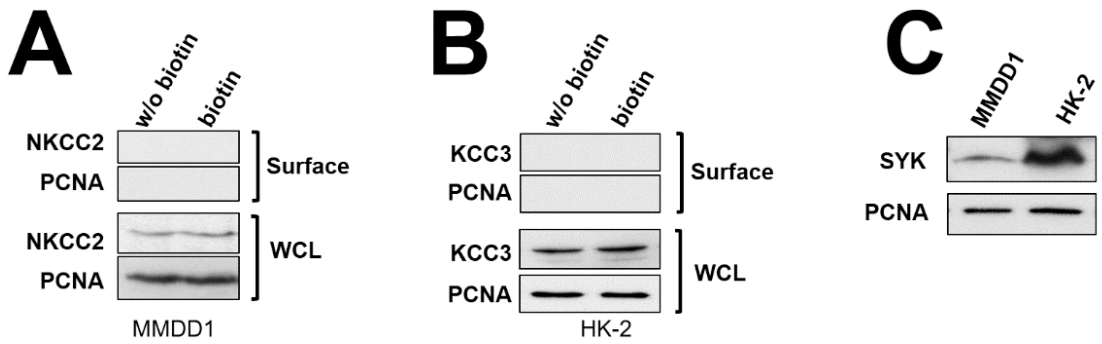

Transporter name	gene	SYK motif
NKCC2	SLC12A1	Y45EET
NKCC1	SLC12A2	
NCC	SLC12A3	
KCC1	SLC12A4	
KCC2	SLC12A5	
KCC3	SLC12A6	Y63EEG
KCC4	SLC12A7	
Cl-/HCO3-exchanger	SLC26A3	
Pendrin	SLC26A4	
Pendrin L1	SLC26A6	
Sulfate Anion Transporter	SLC26A7	
Cl-/HCO3-exchanger	SLC26A9,	
ROMK	KCNJ1	
ENaC- alpha subunit	SCNN1A	
ENaC- beta subunit	SCNN1B	
ENaC- gamma subunit	SCNN1G	
ENaC- delta subunit	SCNN1D	
TRPV4	TRPV4	
TRPV5	TRPV5	
TRPV6	TRPV6	

CFTR	CFTR	Y512DEY